

Radiation-Hydrodynamical Collapse of Pregalactic Clouds in the Ultraviolet Background

T. Kitayama¹, Y. Tajiri², M. Umemura³, H. Susa³ and S. Ikeuchi⁴

¹ *Department of Physics, Tokyo Metropolitan University, Hachioji, Tokyo 192-0397, Japan*

² *Institute of Physics, University of Tsukuba, Tsukuba 305-8577, Japan*

³ *Center for Computational Physics, University of Tsukuba, Tsukuba 305-8577, Japan*

⁴ *Department of Physics, Nagoya University, Chikusa-ku, Nagoya 464-8602, Japan*

11 November 2018

ABSTRACT

To elucidate the effects of the UV background radiation on the collapse of pregalactic clouds, we implement a radiation-hydrodynamical calculation, combining one-dimensional spherical hydrodynamics with an accurate treatment of the radiative transfer of ionizing photons. Both absorption and scattering of UV photons are explicitly taken into account. It turns out that a gas cloud contracting within the dark matter potential does not settle into hydrostatic equilibrium, but undergoes run-away collapse even under the presence of the external UV field. The cloud center is shown to become self-shielded against ionizing photons by radiative transfer effects before shrinking to the rotation barrier. Based on our simulation results, we further discuss the possibility of H₂ cooling and subsequent star formation in a run-away collapsing core. The present results are closely relevant to the survival of subgalactic Population III objects as well as to metal injection into intergalactic space.

Key words: cosmology: theory – diffuse radiation – galaxies: formation – radiative transfer

1 INTRODUCTION

It is widely recognized that the Ultraviolet (UV) background radiation, inferred from the proximity effect of Ly α absorption lines in QSO spectra (e.g., Bajtlik, Duncan & Ostriker 1988; Bechtold 1994; Giallongo et al. 1996), is likely to exert a significant influence upon the collapse of pregalactic clouds and consequently the formation of galaxies. Several authors have argued that the formation of subgalactic objects is suppressed via photoionization and photoheating caused by the UV background (Umemura & Ikeuchi 1984; Ikeuchi 1986; Rees 1986; Bond, Szalay & Silk 1988; Efstathiou 1992; Babul & Rees 1992; Zhang, Anninos & Norman 1995; Thoul & Weinberg 1996). Final states of the photoionized clouds, however, are still unclear, because most of these studies assume optically-thin media, which precludes us from the correct assessment of self-shielding against the external UV fields. Self-shielding not only plays an important role in the thermal and dynamical evolution, but is also essential for the formation of hydrogen molecules (H₂) which control the star formation in metal poor environments such as primordial galaxies. Several attempts have recently been made to take account of the radiative transfer of ionizing photons, adopting for instance a pure absorption approximation (Kepner, Babul & Spergel 1997; Kitayama & Ikeuchi 2000, hereafter KI), the photon conservation method (Abel,

Norman & Madau 1999), and the full radiative transfer treatment (Tajiri & Umemura 1998, hereafter TU; Barkana & Loeb 1999; Susa & Umemura 2000). As for the dynamical states, Kepner, Babul & Spergel (1997) and Barkana & Loeb (1999) have considered *hydrostatic* equilibria of spherical clouds within virialized dark halos. KI have explored the *hydrodynamical* evolution of a spherical system composed of dark matter and baryons. The full radiative transfer treatment, however, has not hitherto been incorporated with the hydrodynamics of spherical pregalactic clouds.

In this paper, we attempt to implement an accurate radiation-hydrodynamical (RHD) calculation on the evolution of spherical clouds exposed to the UV background, solving simultaneously the radiative transfer of photons and the gas hydrodynamics. Our goals are to predict at a physically reliable level final states of photoionized clouds and also to assess accurately self-shielding against the UV background that is essential for H₂ cooling and the subsequent star formation. Throughout the present paper, we assume the density parameter $\Omega_0 = 1$, the Hubble constant $h = H_0/(100 \text{ km s}^{-1} \text{ Mpc}^{-1}) = 0.5$, and the baryon density parameter $\Omega_b = 0.1$.

2 MODEL

A pregalactic cloud is supposed to be a mixture of baryonic gas and dark matter with the mass ratio of $\Omega_b : \Omega_0 - \Omega_b = 1 : 9$. The numerical scheme for the spherical Lagrangian dynamics of two-component matter follows the method described in Thoul & Weinberg (1995) and KI. At each time-step, the radiative transfer is solved with the method devised by TU, in which both absorption and emission (scattering) of ionizing photons are explicitly taken into account. We assume for simplicity that the baryonic gas is composed of pure hydrogen. Neglecting helium causes only a minor effect in the ionization degree less than about the order of 10% (Osterbrock 1989; Nakamoto, Susa & Umemura 1998). We further assume ionization equilibrium among photoionization, collisional ionization, and recombination. This assumption is well justified in the present analysis (see §2.2 of KI for discussion). The number of mass shells is $N_b = 200$ for baryonic gas and $N_d = 2000$ for dark matter. At each radial point, angular integration of the radiative transfer equation is done over at least 20 bins in $\theta = 0 - \pi$, where θ is the angle between the light ray and the radial direction. This is achieved by handling 300 – 700 impact parameters for light rays. The radiation field and the ionization states in the cloud interior are solved iteratively until the HI fraction, X_{HI} , in each mesh converges within an accuracy of 1%.

The external UV field is presumed to be isotropic and to have a power-law spectrum:

$$J(\nu) = J_{21} \left(\frac{\nu}{\nu_{\text{HI}}} \right)^{-\alpha} \times 10^{-21} \text{ erg s}^{-1} \text{ cm}^{-2} \text{ str}^{-1} \text{ Hz}^{-1}, \quad (1)$$

where J_{21} is the intensity at the Lyman edge of hydrogen ($h\nu_{\text{HI}} = 13.6\text{eV}$) and α is the spectral index. We consider two typical cases for α , i.e., $\alpha = 1$ representative for black hole accretion and $\alpha = 5$ for stellar UV sources. Observations of the proximity effect in the Ly α forest suggest $J_{21} = 10^{\pm 0.5}$ at $z = 1.7 - 4.1$ (e.g., Bajtlik, Duncan & Ostriker 1988; Bechtold 1994; Giallongo et al. 1996), but its value is still uncertain at other redshifts. In what follows we give the onset of the UV background to be at $z_{\text{UV}} = 20$ and study the following two cases for J_{21} :

(i) Constant UV

$$J_{21} = 1 \quad z \leq z_{\text{UV}}, \quad (2)$$

(ii) Evolving UV

$$J_{21} = \begin{cases} \exp[-(z-5)] & 5 \leq z \leq z_{\text{UV}} \\ 1 & 3 \leq z \leq 5 \\ \left(\frac{1+z}{4}\right)^4 & 0 \leq z \leq 3. \end{cases} \quad (3)$$

The form of the UV evolution at $z > 5$ in (ii) is roughly consistent with the results of recent models for the reionization of the universe (e.g., Ciardi et al 2000; Umemura, Nakamoto & Susa 2000).

We start the simulations when the overdensity of a cloud is still in the linear regime, adopting the initial and boundary conditions described in KI. The initial overdensity profile is $\delta_i(r) = \delta_i(0) \sin(kr)/kr$, where k is the comoving wave number, and the central overdensity $\delta_i(0)$ is fixed at 0.2. The outer boundary is taken at the first minimum of $\delta_i(r)$, i.e., $kr = 4.4934$, within which the volume averaged overdensity $\bar{\delta}(< r)$ vanishes. Following Haiman, Thoul & Loeb (1996), the characteristic mass of a cloud M_{cloud} is

defined as the baryon mass enclosed within the first zero of $\delta_i(r)$, i.e., $kr = \pi$. Collapse redshift z_c is defined as the epoch at which M_{cloud} would collapse to the center in the absence of thermal pressure. Circular velocity V_c and virial temperature T_{vir} are related to z_c and M_{cloud} via usual definitions:

$$V_c = 15.9 \left(\frac{M_{\text{cloud}} \Omega_0 / \Omega_b}{10^9 h^{-1} \text{ M}_\odot} \right)^{1/3} (1+z_c)^{1/2} \text{ km s}^{-1}, \quad (4)$$

$$T_{\text{vir}} = 9.09 \times 10^3 \left(\frac{\mu}{0.59} \right) \left(\frac{M_{\text{cloud}} \Omega_0 / \Omega_b}{10^9 h^{-1} \text{ M}_\odot} \right)^{2/3} (1+z_c) \text{ K}, \quad (5)$$

where μ is the mean molecular weight in units of the proton mass m_p .

The collapse of a gas shell is traced until it reaches the rotation radius specified by the dimensionless spin parameter;

$$r_{\text{rot}} = 0.05 \left(\frac{\Omega_b / \Omega_0}{0.1} \right)^{-1} \left(\frac{\lambda_{\text{ta}}}{0.05} \right)^2 r_{\text{ta}}, \quad (6)$$

where r_{ta} is the turnaround radius of the gas shell, and we adopt a median for the spin parameter, $\lambda_{\text{ta}} = 0.05$ (Efstathiou & Jones 1979; Barns & Efstathiou 1987; Warren et al. 1992). Below the size given by (6), the system would attain rotational balance and forms a disk eventually.

3 RESULTS

3.1 Significance of radiative transfer

To demonstrate the significance of coupling the radiative transfer of ionizing photons with hydrodynamics, we first present in Fig. 1 estimations for relevant timescales at the center of a uniform static cloud with circular velocity V_c and collapse epoch z_c , where the external UV is specified by J_{21} and a spectral index α . The photoionization timescale t_{ion} and the photoheating timescale t_{heat} are compared to the dynamical timescale t_{dyn} , either by solving the radiative transfer of UV photons through the cloud or by just assuming the optically thin medium. Wherever necessary, we have adopted the temperature $T = 10^4 \text{ K}$, the proton number density $n_{\text{H}} = n_{\text{H}}^{\text{vir}} = 5.0 \times 10^{-5} (\Omega_b h^2 / 0.025) (1+z_c)^3 \text{ cm}^{-3}$, the mass density $\rho = m_p n_{\text{H}} \Omega_0 / \Omega_b$, and the radius $R = R_{\text{vir}} = 64 (V_c / 30 \text{ km s}^{-1}) (\Omega_0 h^2 / 0.025)^{-1/2} (1+z_c)^{-3/2} \text{ kpc}$. In the low-density limit, the contours of $t_{\text{ion}} = t_{\text{dyn}}$ and $t_{\text{heat}} = t_{\text{dyn}}$ both approach asymptotically the optically thin case $J_{21} \propto \sqrt{n_{\text{H}}^{\text{vir}}} \propto (1+z_c)^{3/2}$. The differences originated from the cloud sizes are rather small compared to those arisen when one incorporates the radiative transfer or not.

Fig. 1 predicts that the significance of radiative transfer effects increases with increasing redshift (i.e., increasing cloud density) and decreasing J_{21} for a given α . Under the UV evolution given in equation (3), for example, $t_{\text{dyn}} < t_{\text{ion}}$ and $t_{\text{dyn}} < t_{\text{heat}}$ are satisfied at the center of a cloud with $V_c = 30 \text{ km s}^{-1}$ at $z_c \gtrsim 10$, and the cloud is shielded against the external radiation in terms of photoionization as well as photoheating. At $6 \lesssim z_c \lesssim 10$, $t_{\text{heat}} < t_{\text{dyn}} < t_{\text{ion}}$ is achieved, indicating that the cloud center is heated but not ionized by the UV radiation (Gnedin & Ostriker 1997; KI). Contrastively, both t_{ion} and t_{heat} become shorter than t_{dyn}

at $z_c < 6$ and the cloud is likely to evolve in a similar fashion to the optically-thin case. We can see qualitatively the same relations for $\alpha = 5$, except that shielding of ionization and heating occurs almost simultaneously at lower redshift. It should be noted that the above estimations are made for a virialized cloud using the UV intensity only at z_c . As shown in forthcoming sections, the central density of a collapsing cloud actually continues to ascend to above $n_{\text{H}}^{\text{vir}}$ and the radiative transfer effects can become important even at low redshifts. In addition, possible changes of the UV intensity during the dynamical growth of a cloud can also affect its ionization structure.

3.2 Dynamical evolution

Fig. 2 shows the dynamical evolution of a cloud with $V_c = 29 \text{ km s}^{-1}$ under the constant UV background at $z < z_{\text{UV}} = 20$. This cloud would collapse at $z_c = 3$ if there were no UV background. In practice, the cloud turns around and contracts in the inner parts, while it continues to expand in the outer envelope. For a hard UV spectrum with $(J_{21}, \alpha) = (1, 1)$, the gas is ionized and heated up to $T \sim 10^4 \text{ K}$ promptly at the onset of the UV background. For a soft UV spectrum with $(J_{21}, \alpha) = (1, 5)$, the cloud center is kept self-shielded against the external field and the temperature ascends more gradually.

For comparison, results of the optically-thin and pure absorption calculations are also presented in Fig. 2. The pure absorption case is based on the analytical formalism described in KI. The cloud evolution is altered in no small way by different treatments of the UV radiation. Under the optically-thin assumption, the cloud is completely prohibited from collapsing for $(J_{21}, \alpha) = (1, 1)$, and from being self-shielded for $(J_{21}, \alpha) = (1, 5)$. The pure absorption approximation leads to accelerating the collapse of the central core and to underestimating photoionization and photoheating.

Fig. 3 exhibits the radial profiles of the same clouds at $z = 3$ for $(J_{21}, \alpha) = (1, 5)$. The inner part of a cloud does not settle into hydrostatic equilibrium, but rather undergoes isothermal run-away collapse and the density profile follows the self-similar solution of Bertschinger (1985). The trend is regardless of the treatment of the UV radiation transfer, because the temperature of thermal equilibrium in optically-thin media comes close to 10^4 K in the high density limit. The present results demonstrate that the approximation of hydrostatic equilibrium employed in previous analyses (Kepner, Babul & Spergel 1997; Barkana & Loeb 1999) breaks down for the final states.

The ionization structure is quite different depending on whether one incorporates the radiative transfer or not. In an optically-thin cloud, the ionization degree changes merely according to the ionization parameter, n_{H}/J_{21} , whereas the radiative transfer effects produce a self-shielded neutral core (Fig. 3c). Fig. 3(d) further indicates that the UV heating rate is reduced significantly in the self-shielded region, with an increasing contribution of scattered photons to the total heating rate. Implications of the present results on H_2 cooling [thin lines in panel (d)] will be discussed in detail in Sec 4.

Effects of the evolution of the UV background are illustrated in Fig. 4. Due to very low UV intensity at high red-

shift, the whole cloud is kept self-shielded in terms of both photoionization and photoheating at $z \gtrsim 12$. For a cloud with relatively high z_c ($z_c = 4.8$, Fig. 4a), the cloud center begins to contract before the penetration of the external UV. Hence, the dynamical evolution closely coincides with that without the UV background. As the virial temperature of the cloud is $T_{\text{vir}} \sim 3 \times 10^4 \text{ K}$, the cloud center is shock-heated to above 10^4 K and cools via atomic cooling. On the other hand, a cloud with low z_c ($z_c = 0.5$, Fig. 4b) is once photoionized to the similar level to the constant UV case at $3 < z < 5$, but is able to collapse as the UV intensity drops at lower redshifts.

3.3 Criteria for collapse

Figs 5 and 6 summarize the results of present calculations for a variety of initial conditions on a $V_c - z_c$ plane. As our simulations assume ionization equilibrium and only incorporate atomic cooling, they can be most securely applied to a cloud once heated to above 10^4 K either by shock or by UV photons during the course of its evolution. In contrast, evolution of lower temperature systems is still tentative and may be altered once cooling by molecular hydrogen is explicitly taken into account. These figures thus distinguish “high temperature clouds” (circles) defined as those photoheated to $> 10^4 \text{ K}$ or those with $T_{\text{vir}} > 10^4 \text{ K}$, and the other “low temperature clouds” (triangles). Each of these populations are further classified by open and filled symbols depending on whether or not they collapse to the rotation barrier within the present age of the universe.

It is obvious that the UV background prohibits small clouds from collapsing even if the transfer of ionizing photons is considered. Under a constant UV flux (Fig. 5), threshold circular velocity for the collapse gradually increases with decreasing redshift, i.e., decreasing cloud density. The threshold velocity also decreases with increasing photon spectral index α because of the smaller number of high energy photons. At $z_c \gtrsim 5$, the threshold falls below 10^4 K , because the cloud center starts to contract before the onset of the UV background and remains impervious to the external photons. In the presence of the UV evolution (Fig. 6), the threshold velocity increases sharply at $z_c \lesssim 3$ and drops slightly at $z_c \lesssim 1$. The central temperature of a cloud denoted by an open triangle can reach $\sim 10^4 \text{ K}$ by adiabatic compression and the collapse is promoted by atomic cooling. A cloud denoted by a filled triangle fails to collapse because of the lack of coolant at $T < 10^4 \text{ K}$ in our simulations. As will be discussed in Sec 4, however, evolution of these “low temperature clouds” may be modified by H_2 cooling.

KI have suggested that the threshold for collapse is roughly determined by the balance between the gravitational force and the thermal pressure gradient when the gas is maximally exposed to the external UV flux. To confirm this, we plot in the same figures a relation $T_{\text{vir}} = T_{\text{eq}}^{\text{max}}$, where $T_{\text{eq}}^{\text{max}}$ is the maximum equality temperature defined semi-analytically as follows. Firstly, given the initial overdensity profile, the collapse of a spherical perturbation is approximated by the self-similar solution of Bertschinger (1985). Secondly, at an arbitrary stage of the collapse, one can compute the equality temperature at which radiative cooling balances photoheating in the optically thin limit,

using the central density deduced from the self-similar solution and the UV intensity assumed in the simulation. Finally, $T_{\text{eq}}^{\text{max}}$ is set equal to the maximum of such temperature. For the gas exposed to a constant UV flux from the linear regime, $T_{\text{eq}}^{\text{max}}$ is attained essentially at turn-around. If a cloud has T_{vir} above $T_{\text{eq}}^{\text{max}}$, it is likely to be gravitationally unstable against gas pressure.

Figs 5 and 6 show that the above criteria agree reasonably well with our simulation results based on the accurate treatment of the radiative transfer. This is because the dynamical evolution is basically regulated by the Jeans criterion when a cloud is heated up to $\sim 10^4\text{K}$ by the UV background before contraction. At high redshifts ($z_c \gtrsim 6$ in Fig. 5 and $z_c \gtrsim 3$ in Fig. 6), however, the cloud center is strongly self-shielded from early stages and the approximation of the optically thin limit breaks down. The Jeans scale at these epochs is reduced below the relation $T_{\text{vir}} = T_{\text{eq}}^{\text{max}}$.

4 IMPLICATIONS FOR GALAXY FORMATION IN THE UV BACKGROUND

The present RHD calculations give an accurate prediction for the suppression of pregalactic collapse due to the UV background, which has been one of the primary concerns from the viewpoint of galaxy formation (Umemura & Ikeuchi 1984; Ikeuchi 1986; Rees 1986; Bond, Szalay & Silk 1988; Efsthathiou 1992; Babul & Rees 1992; Zhang, Anninos & Norman 1995; Thoul & Weinberg 1996; KI). What is of additional significance in this context is the subsequent formation of stars in collapsing clouds. In order for stars to form, a cloud needs to be cooled down to below 10^4K by hydrogen molecules, because they are the only coolant in metal-deficient gas (e.g., Peebles & Dicke 1968; Matsuda, Sato & Takeda 1969; Tegmark et al. 1997). H_2 cooling is a two-body collision process (e.g., Hollenbach & McKee 1989; Galli & Palla 1998), while the photoheating rate is in proportion to the density. The potentiality of H_2 cooling is therefore enhanced with increasing density. In this respect, run-away collapse should provide favorable situations for H_2 cooling.

Based on our simulation results presented in the previous section, we further investigate the possibility of star formation in a collapsing core. We suppose that cooling below 10^4K becomes efficient if the following two conditions are both satisfied; 1) photodissociation of molecular hydrogen by the UV photons in the Lyman-Werner bands at 11.26–13.6keV (e.g., Stecher & Williams 1967) is less important than other H_2 destruction processes, and 2) H_2 cooling overtakes UV photoheating. The first condition is fulfilled for clouds heated up to $> 10^4\text{K}$, because destruction of H_2 is dominated by collisional dissociation insofar as $T \gtrsim 2000\text{K}$ (Corbelli, Galli & Palla 1997). More specifically, requiring that the timescale of H_2 dissociation via collisions with H^+ (reaction 12 of Shapiro & Kang 1987) is shorter than that of photodissociation (Draine & Bertoldi 1996; Omukai & Nishi 1999) in the conservative optically thin limit, we have for the electron density

$$n_e > 4.7 \times 10^{-5} \left(\frac{13.6}{12.4} \right)^\alpha J_{21} \exp(21200 \text{ K}/T) \text{ cm}^{-3}, \quad (7)$$

which is amply satisfied at the collapsing core of our simulated clouds. The second condition depends on the amount

of H_2 formed. In the absence of the external UV field, the H_2 abundance in the metal-deficient postshock layer converges roughly to $X_{\text{H}_2} \approx 10^{-3}$ (e.g., Shapiro & Kang 1987; Ferrara 1998; Susa et al. 1998). Under the UV field, $X_{\text{H}_2} \approx 10^{-3}$ is also achieved if photoheating is strongly attenuated by self-shielding, while the abundance is reduced down to $X_{\text{H}_2} \approx 10^{-6}$ in the case of weak attenuation of photoheating (Kang & Shapiro 1992; Corbelli et al. 1997; Susa & Umemura 2000; Susa & Kitayama 2000). It is also likely that the H_2 abundance depends on the spectrum of the impinging radiation and the details of the ionizing structure of the medium (e.g., Kang & Shapiro 1992; Ciardi et al. 2000). Leaving such complexities elsewhere (Kitayama et al. in preparation), we make crude estimations for the cooling rate using the H_2 cooling function of Hollenbach & McKee (1989) and assuming $X_{\text{H}_2} = 10^{-3}$ in the full transfer and pure absorption cases, and $X_{\text{H}_2} = 10^{-6}$ in the optically thin case.

Fig. 3(d) shows that H_2 cooling greatly overwhelms photoheating in the self-shielded neutral core for $X_{\text{H}_2} = 10^{-3}$. It turns out that what enables H_2 cooling to be effective is essentially the attenuation of photoheating rather than the final abundance of H_2 molecules. In fact, in the strongly self-shielded core, H_2 cooling remains to be dominant even if the abundance is reduced to a level similar to the optically-thin case, i.e., $X_{\text{H}_2} = 10^{-6}$ (the H_2 cooling rate is roughly proportional to X_{H_2} at $T \lesssim 10^4 \text{ K}$). We have further checked that this is the case with every collapsed cloud plotted as an open circle in Figs 5 and 6. Under the optically-thin approximation, on the other hand, UV heating is much stronger than H_2 cooling, prohibiting the cooling below 10^4K .

While the above arguments support the possibility of H_2 cooling during the collapse of “high temperature clouds” (open circles in Figs 5 and 6), the situation is rather intricate for “low temperature clouds” (triangles in the same figures). Once incorporated formation and destruction of molecular hydrogen explicitly in our calculations, these clouds would be able to collapse as long as the external UV flux is negligible or very weak. For somewhat stronger UV flux, photodissociation may operate efficiently to suppress H_2 formation and to prohibit the collapse (Haiman, Rees & Loeb 1996, 1997; Haiman, Abel & Rees 2000; Ciardi et al. 2000). Alternatively, self-shielding induced by run-away collapse may still enable a sufficient amount of H_2 to be formed for the system to cool down to $\sim 100\text{K}$. These points will be investigated thoroughly in our future work (Kitayama et al. in preparation).

In summary, self-shielding against the UV background is indispensable for H_2 cooling and subsequent star formation to proceed. Run-away collapse is likely to promote clouds with $T_{\text{vir}} > 10^4\text{K}$ to cool down before collapsing to the rotation barrier given by equation (6). These results are closely relevant to the formation of dwarf galaxies at high redshifts as well as to metal injection into intergalactic space (e.g., Nishi & Susa 1999). Note that the above conclusions do not conflict with those of several recent works (Haiman, Rees & Loeb 1996, 1997; Ciardi et al. 2000; Haiman et al. 2000) that the so called “radiative feedback” is operating in the early universe and suppresses the collapse of some objects via photodissociation of H_2 molecules. Current simulations are mainly aimed to study the clouds once heated to above 10^4K either by shock or by UV photons, for which

photodissociation has minor impacts on H_2 formation compared to collisional dissociation (eq. [7]). In addition, run-away collapse yields a highly self-shielded core which is particularly favorable for H_2 formation. Photodissociation may be of greater significance in smaller clouds and lower density regions.

Finally, we discuss the effects of the geometry of cloud evolution upon H_2 cooling. Near and above the Jeans scale, clouds are expected to contract spherically to a first order approximation and result in run-away collapse as shown in the present paper. Clouds far above the Jeans scale, on the other hand, are likely to undergo pancake collapse. The pancakes would not end up with run-away collapse, because the gravity of the sheet is readily overwhelmed by the pressure force. Susa & Umemura (2000) have explored pregalactic pancake collapse including the UV transfer and H_2 formation, and shown that the collapsing pancakes bifurcate, depending upon the initial masses, into less massive UV-heated ones and more massive cooled ones. This is because the self-shielding in sheet collapse is governed by the column density of a pregalactic cloud. To conclude, star formation in pregalactic clouds in the UV background is strongly regulated by the behaviour of collapse and the manner of the radiation transfer.

ACKNOWLEDGMENTS

We thank Andrea Ferrara for helpful comments, Taishi Nakamoto for discussions, and Susumu Inoue for careful reading of the manuscript. This work is supported in part by Research Fellowships of the Japan Society for the Promotion of Science for Young Scientists, No. 7202 (TK) and 2370 (HS).

REFERENCES

- Abel T., Norman M. L., Madau P., 1999, *ApJ*, 523, 66
 Babul A., Rees M. J., 1992, *MNRAS*, 255, 346
 Bajtlik S., Duncan R. C., Ostriker J. P., 1988, *ApJ*, 327, 570
 Barkana R., Loeb A., 1999, 523, 54
 Barns J., Efstathiou G., 1987, *ApJ*, 319, 575
 Bechtold J., 1994, *ApJS*, 91, 1
 Bertschinger E., 1985, *ApJS*, 58, 39
 Bond J. R., Szalay A. S., Silk J., 1988, *ApJ*, 324, 627
 Ciardi B., Ferrara A., Governato F., Jenkins A., 2000, *MNRAS*, submitted
 Corbelli E., Galli D., Palla F., 1997, *ApJ*, 487, L53
 Efstathiou G., 1992, *MNRAS*, 256, 43
 Efstathiou G., Jones B. J. T., 1979, *MNRAS*, 186, 133
 Ferrara, A., 1998, *ApJ*, 499, L17
 Galli D., Palla F., 1998, *A&A*, 335, 403
 Giallongo E., Cristiani S., D'Odorico S., Fontana A., Savaglio S., 1996, *ApJ*, 466, 46
 Gnedin N. Y., Ostriker J. P., 1997, *ApJ*, 486, 581
 Haiman Z., Abel T., Rees M. J., 2000, *ApJ*, in press (astro-ph/9903336)
 Haiman Z., Rees M. J., Loeb A., 1996a, *ApJ*, 467, 522
 Haiman Z., Rees M. J., Loeb A., 1997, *ApJ*, 476, 458
 Haiman Z., Thoul A. A., Loeb A., 1996b, *ApJ*, 464, 523
 Hollenbach D., Mckee C. F., 1989, *ApJ*, 342, 306
 Ikeuchi S., 1986, *ApSS*, 118, 509
 Kang H., Shapiro P., 1992, *ApJ*, 386, 432
 Kepner J., Babul A., Spergel N., 1997, *ApJ*, 487, 61
 Kitayama T., Ikeuchi S., 2000, *ApJ*, 529, 615
 Matsuda T., Sato H., Takeda H. 1969, *Prog.Theor.Phys.* 42, 219
 Nakamoto T., Susa H., Umemura M., 1998, in *Proc. Int. Symp. on Supercomputing, New Horizon of Computational Science*, Dordrecht, Kluwer, in press
 Nishi R., Susa H., 1999, *ApJ*, 523, L103
 Omukai K., Nishi R., 1999, *ApJ*, 518, 64
 Osterbrock D. E., 1989, *Astrophysics of Gaseous Nebulae and Active Galactic Nuclei*, Mill Valley, University Science Books
 Peebles P. J. E., Dicke R. H., 1968, *ApJ*, 154, 891
 Rees M. J., 1986, *MNRAS*, 218, 25P
 Shapiro P. R., Kang H., 1987, *ApJ*, 318, 32
 Stecher T. P., Williams D. A., 1967, *ApJ*, 149, L29
 Susa H., Kitayama T., 2000, *MNRAS* submitted
 Susa H., Umemura M., 2000, *ApJ* in press (astro-ph/0001169)
 Susa H., Uehara H., Nishi R., Yamada, M., 1998, *Prog. Theor. Phys.*, 100, 63
 Tajiri Y., Umemura M., 1998, *ApJ*, 502, 59(TU)
 Tegmark M., et al., 1997, *ApJ*, 474, 1
 Thoul A. A., Weinberg D. H., 1995, *ApJ*, 442, 480
 Thoul A. A., Weinberg D. H., 1996, *ApJ*, 465, 608
 Umemura M., Ikeuchi S., 1984, *Prog. Theor. Phys.*, 72, 47
 Umemura M., Nakamoto T., Susa H., 2000, in *Proc. of the 4th RESCEU International Symposium on the Birth and Evolution of the Universe*, Universal Academy Press, in press
 Warren M. S., Quinn P. J., Salmon J. K., Zurek W. H., 1992, *ApJ*, 399, 405
 Zhang Y., Anninos P., Norman M. L., 1995, *ApJ*, 453, L57

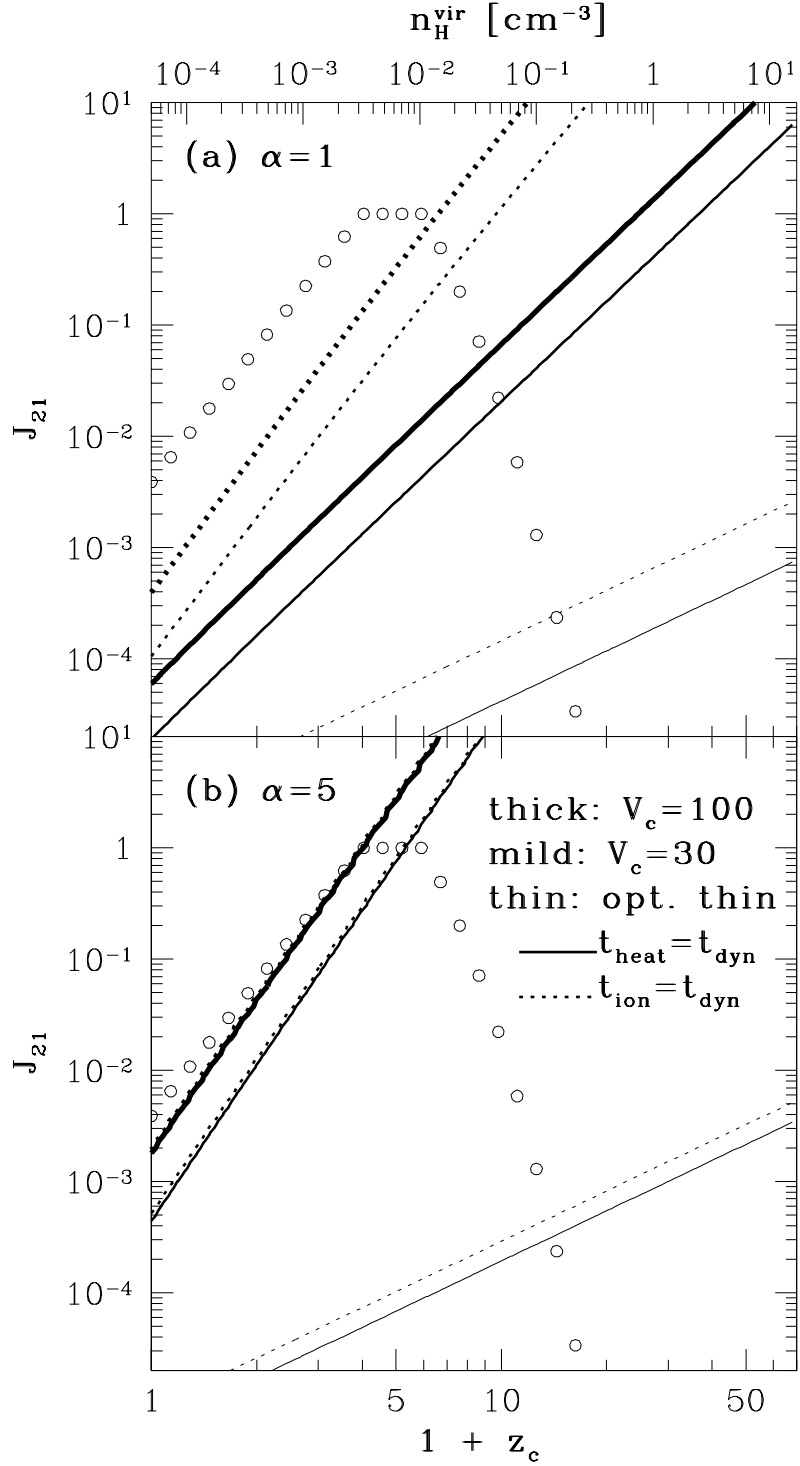


Figure 1. $J_{21} - z_c$ diagram on timescales relevant to the evolution of a pregalactic cloud in the UV background with (a) $\alpha = 1$ and (b) $\alpha = 5$. The photoionization time t_{ion} , the photoheating time t_{heat} , and the dynamical time t_{dyn} are evaluated at the center of a stationary uniform cloud with V_c and z_c as described in the text. Lines indicate the contours $t_{\text{ion}} = t_{\text{dyn}}$ (dotted) and $t_{\text{heat}} = t_{\text{dyn}}$ (solid) for $V_c = 100 \text{ km s}^{-1}$ (thick), 30 km s^{-1} (mildly thick), and in the optically thin limit (thin). In the region under these contours, t_{dyn} becomes shorter than t_{ion} and t_{heat} , respectively. For reference, the track of the UV evolution given in equation (3) is marked by open circles.

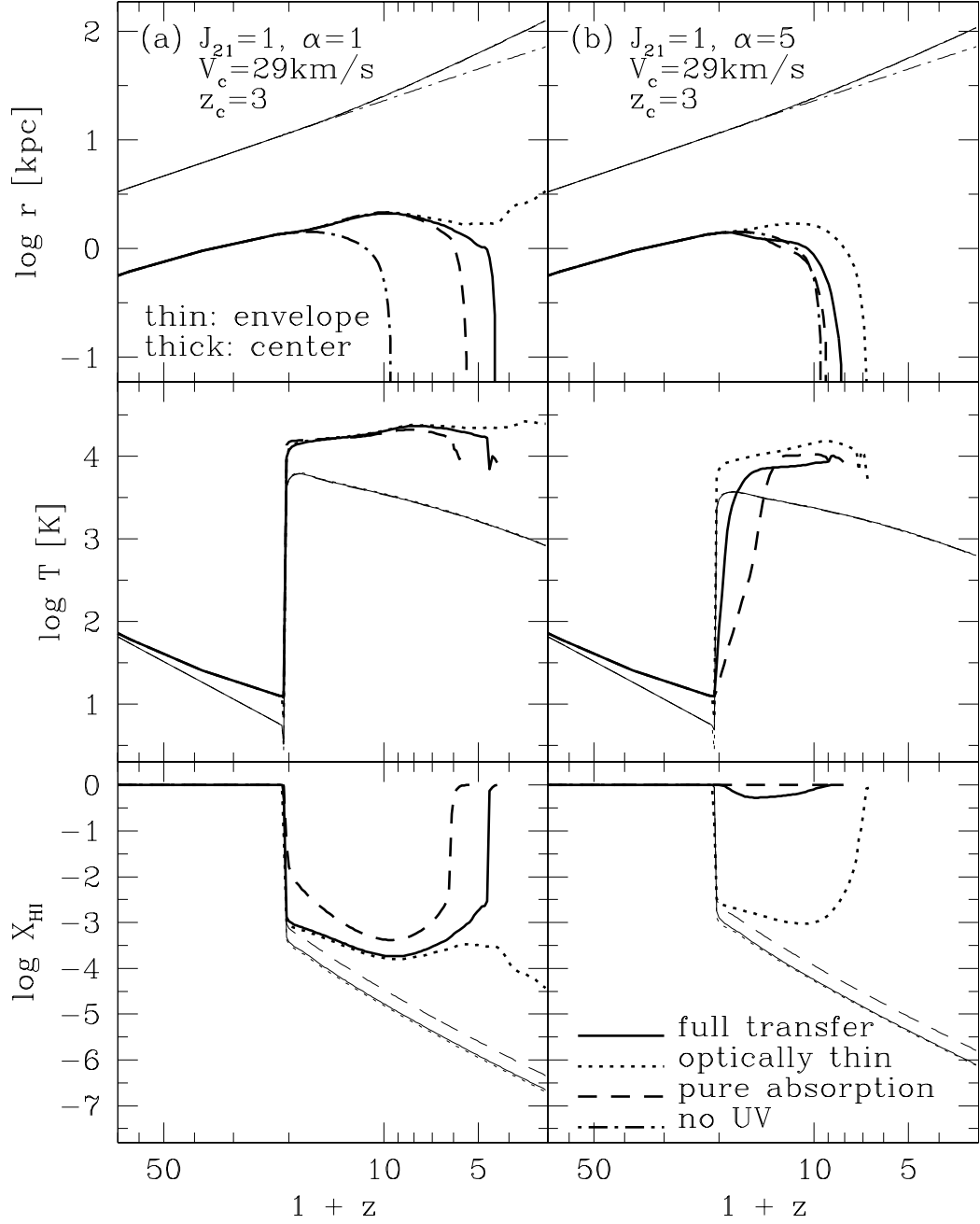


Figure 2. Evolution of radius (top panels), temperature (middle panels), and HI fraction (bottom panels) of gas shells enclosing 0.5% (thick lines) and 90% (thin lines) of total gas mass in a cloud with $V_c = 29$ km/s and $z_c = 3$ under the constant UV background; (a) $(J_{21}, \alpha) = (1, 1)$ and (b) $(1, 5)$. Different line types indicate the full transfer (solid), optically-thin (dotted), and pure absorption (dashed) cases, respectively. Also plotted in the top panels are the no UV (dot-dashed) results.

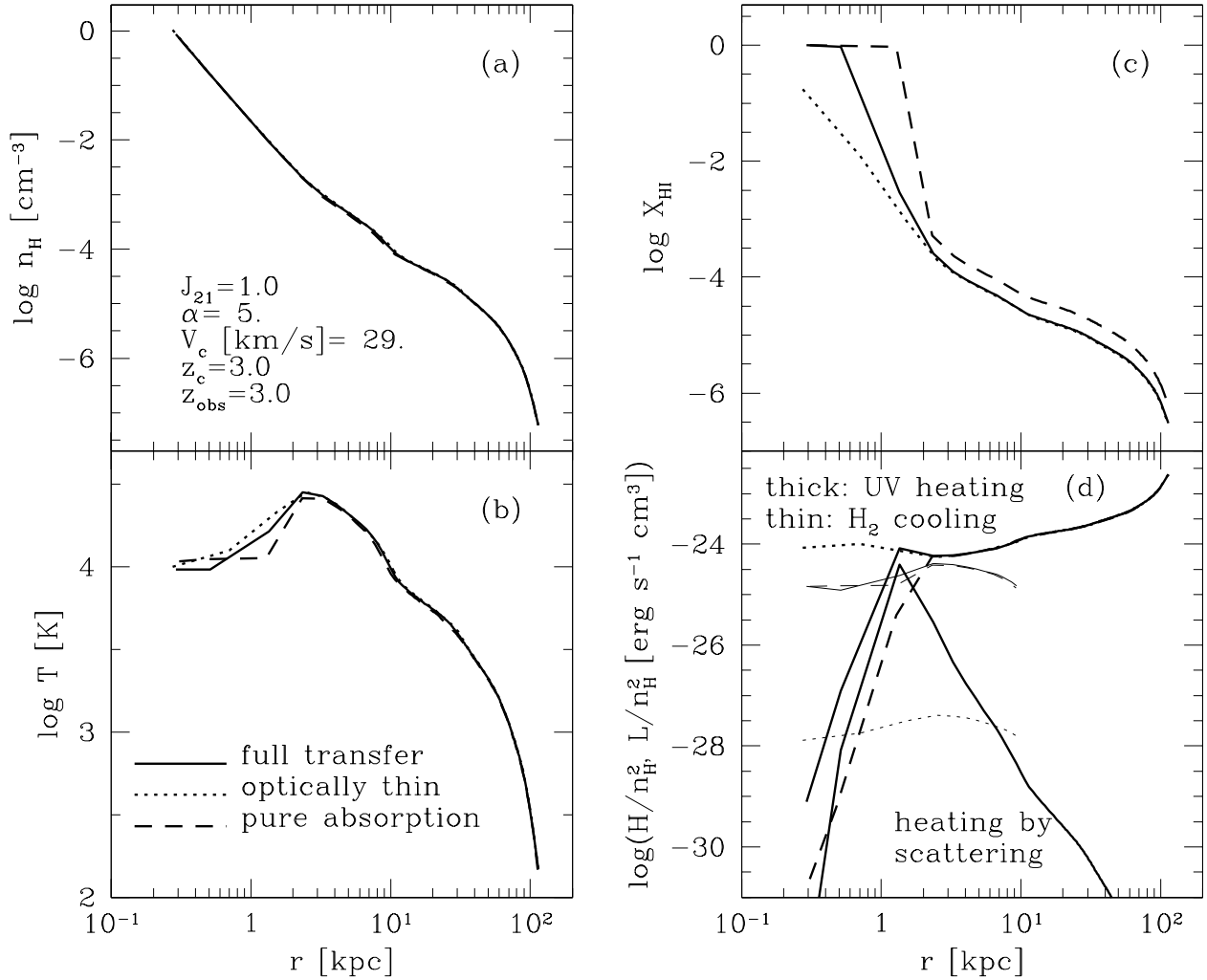


Figure 3. Radial profiles at $z = 3$ of (a) hydrogen density, (b) temperature, (c) HI fraction, and (d) UV heating rate, for $(J_{21}, \alpha) = (1, 5)$, $V_c = 29$ km/s, and $z_c = 3$. Different line types indicate the full transfer (solid), optically-thin (dotted), and pure absorption (dashed) cases, respectively. The heating rate caused by scattering in the full transfer case is added to panel (d). Also plotted in (d) are estimations for the H_2 cooling rate inside the shock front at $r \sim 10$ kpc, assuming $X_{\text{H}_2} = 10^{-3}$ in the full transfer or pure absorption cases, and $X_{\text{H}_2} = 10^{-6}$ in the optically-thin case.

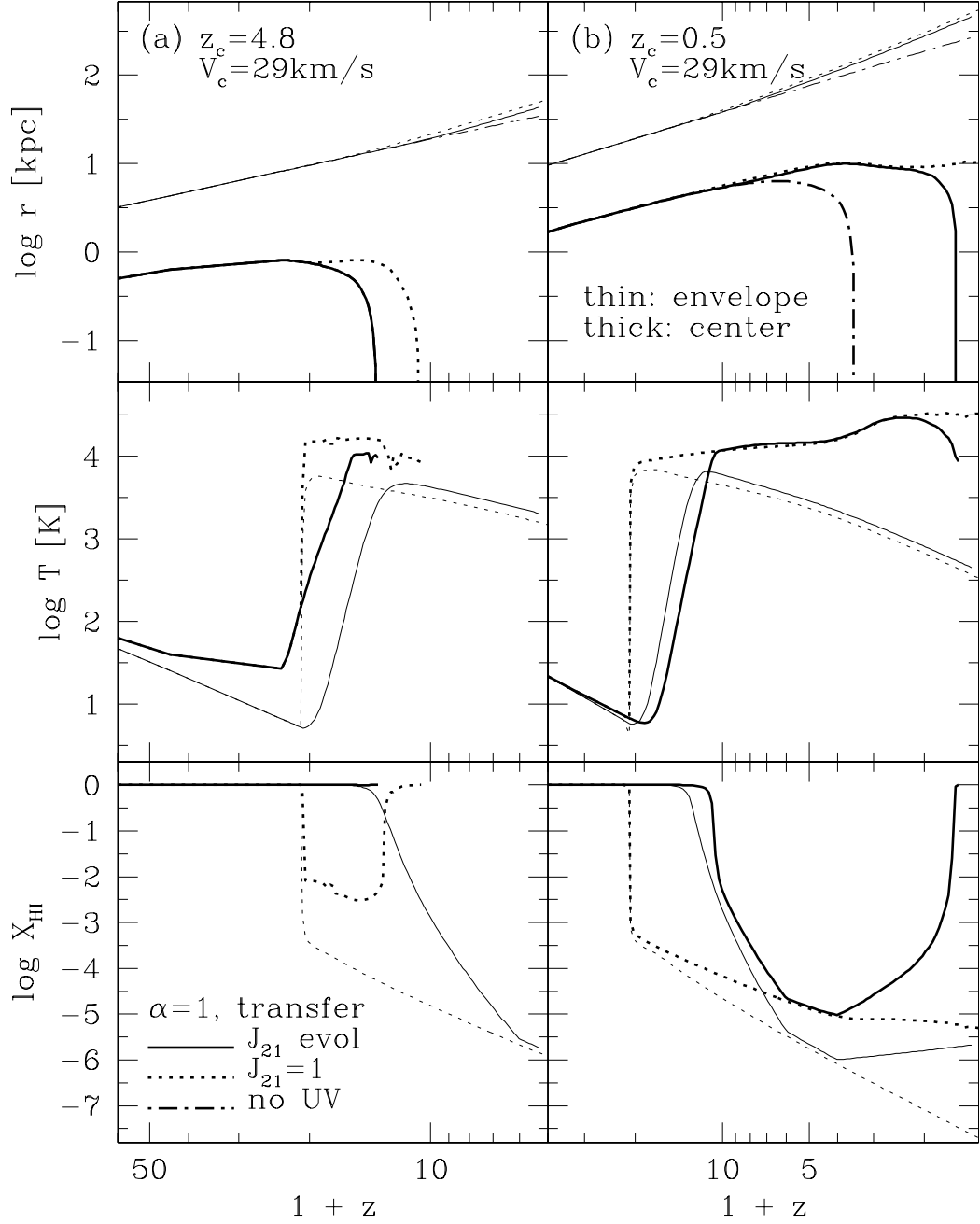


Figure 4. Similar to Fig. 2 except that the effects of the UV evolution (solid lines) are illustrated in comparison to the constant UV (dotted) and no UV (dot-dashed) cases; (a) $z_c = 4.8$, $V_c = 29 \text{ km/s}$, and (b) $z_c = 0.5$, $V_c = 29 \text{ km/s}$. Full transfer results are plotted assuming $\alpha = 1$.

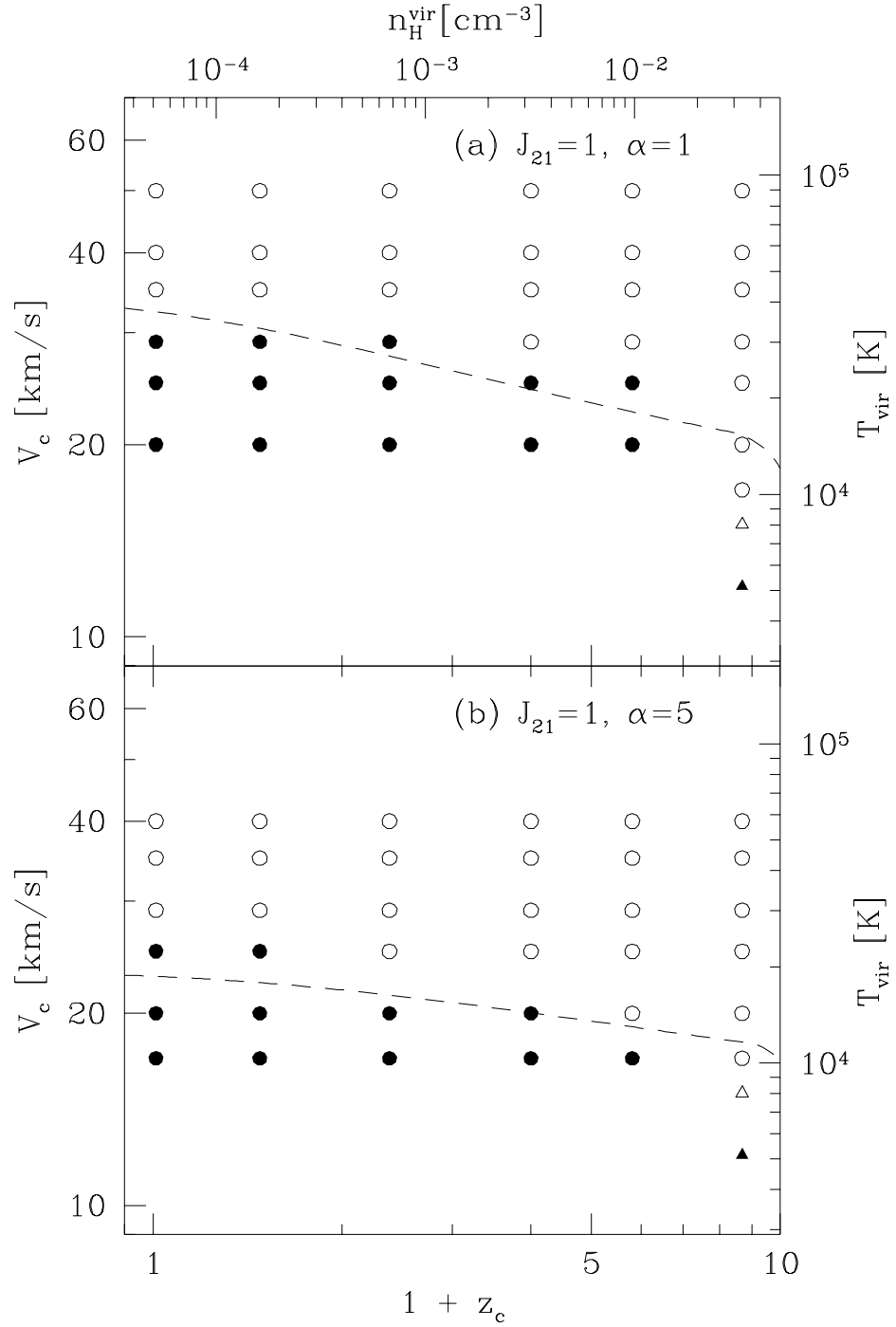


Figure 5. $V_c - z_c$ diagram describing collapse and self-shielding from our full-transfer RHD calculations; (a) $(J_{21}, \alpha) = (1, 1)$, and (b) $(1, 5)$. Circles are the present secure results for “high temperature clouds” and triangles are the tentative results for “low temperature clouds” (see text for definitions). Filled circles are clouds which are prohibited to collapse due to the UV heating, and open circles are those which undergo run-away collapse with $T_{\text{vir}} > 10^4 \text{ K}$. Filled triangles are clouds which cannot collapse to the rotation barrier, and open triangles are those which collapse due to atomic cooling. Also plotted by dashed lines are the relation $T_{\text{vir}} = T_{\text{eq}}^{\text{max}}$ defined in the text.

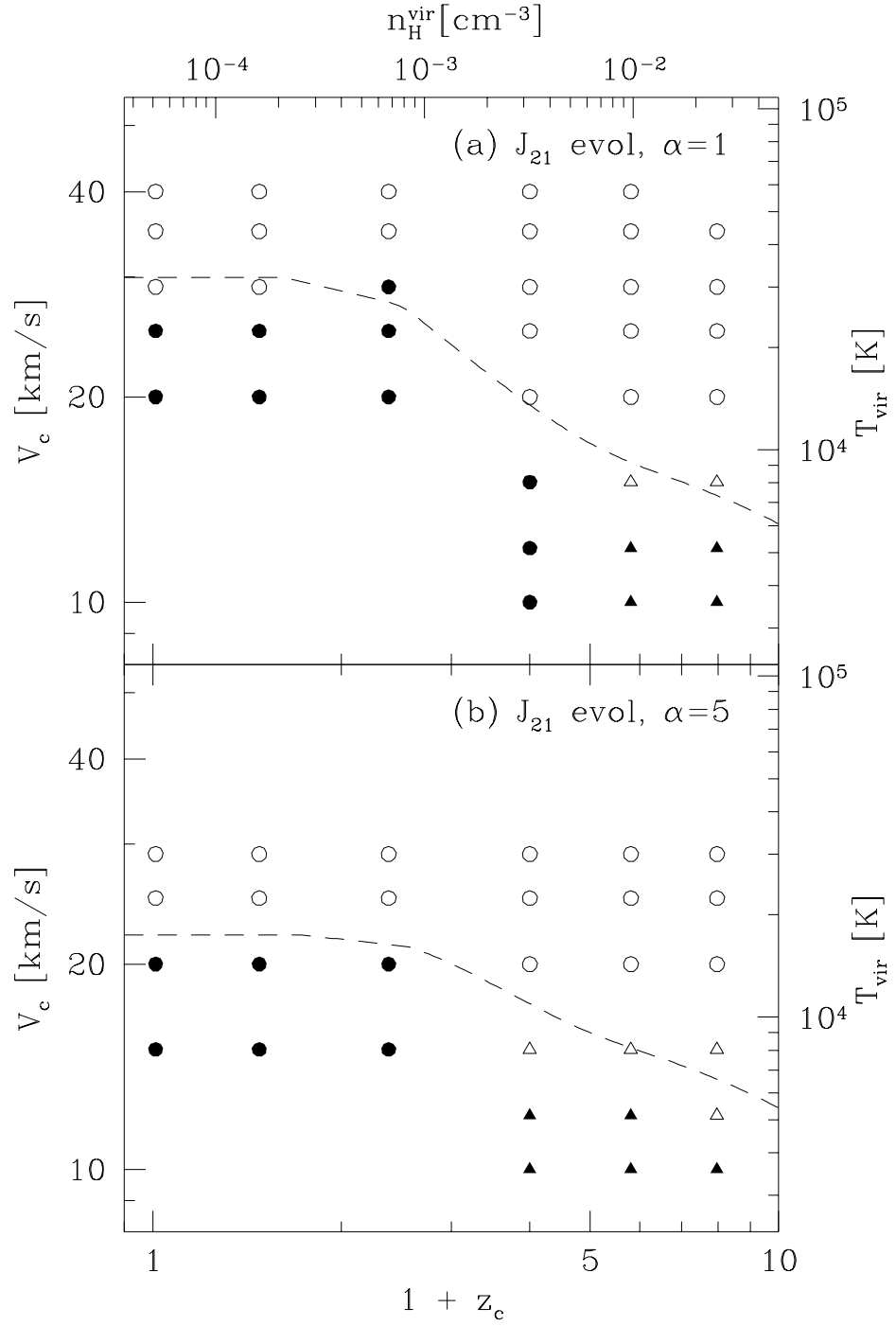


Figure 6. Same as Fig. 5 except that the UV evolution is taken into account.